Analyses of turbulence structures in shear flows

By M. J. LEE

Outline of the research program and a recent progress in the studies of sheared turbulence are described. The research program reported here is directed at two goals: (i) understanding of fundamental physics of organized structures in turbulent shear flows; and (ii) development of phenomenological models of turbulence based on physical arguments. Three projects that have been carried out are:

A. structure of sheared turbulence near a plane boundary;
B. distortion of turbulence by axisymmetric strain and dilatation;
C. study of energy transfer in turbulent shear flow.

1. Motivation and Objectives

Project **A** was motivated by the demonstration of remarkable similarity between homogeneous turbulent shear flow and turbulent channel flow in instantaneous velocity (and vorticity) fields and statistical correlations at the same dimensionless shear rate $S^* = Sq^2/\epsilon$ (Lee, Kim & Moin 1987). Here, $S = dU/dy$ is the mean 'shear rate,' $q^2 = \overline{u_i u_i}$ is twice the turbulent kinetic energy and ϵ is the dissipation rate of the kinetic energy. The similarity in instantaneous vector flow topology as well as in statistical measures bears a profound implication towards a possibility of developing a 'universal' turbulence model. In particular, this study showed that shear rate alone (without a wall) can produce the streaky structures, providing a strong support for the importance of shear rate in determining turbulence structures.

The presence of a solid boundary affects turbulence in two fundamental ways:
(i) generation of mean velocity gradient (via the no-slip condition) which, upon interaction with turbulence, supplies energy to it; and
(ii) suppression of velocity fluctuations in its vicinity.

It is hypothesized that these two effects are distinct in affecting turbulence structure so that they can be accounted for separately. Project **A** centers on the analysis of these two functions of a solid boundary and consists of three subprojects: uniform-shear boundary layer (USBL), plane Couette flow (PCF) and shear-free channel flow (SFCF). See figure 1 for schematic of the flows.

The uniform-shear boundary layer (USBL) project aims at a theoretical explanation of the generation mechanism of the streaks in turbulent shear flows (Lee & Hunt 1988). In USBL, the mean flow has a velocity profile $U = Sy + U_0$ with the shear rate S uniform and constant, and the flow field is assumed to be inviscid with a slip velocity condition at the surface $y = 0$. The analysis was

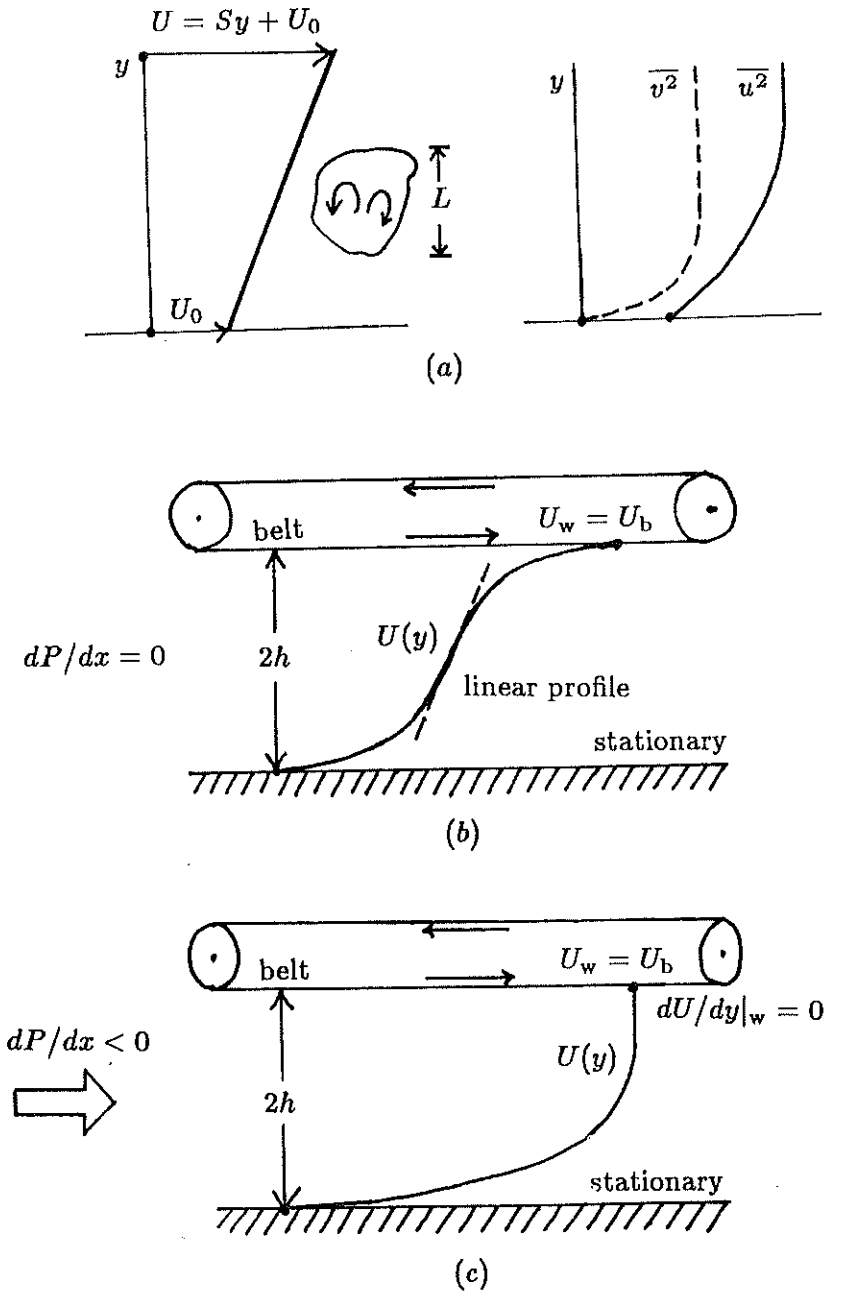

FIGURE 1. Schematic diagram of turbulent shear flows: (*a*) a uniform-shear boundary layer (USBL); (*b*) plane Couette flow (PCF); (*c*) shear-free channel flow (SFCF).

carried out for the evolution and distribution of turbulence by using rapid distortion theory (RDT). Particular emphasis is placed on the differences between the shear-free boundary layer (see Uzkan & Reynolds 1967; Hunt & Graham 1978; Hunt 1984) in redistributing turbulence near the surface by the blocking effect.

The plane Couette flow (PCF) and shear-free channel flow (SFCF) projects were motivated by a need to generate numerical databases of turbulent wall-bounded flows with a constant total shear stress $\tau(y) = \mu dU/dy - \rho\overline{uv} = \tau_w$ across the boundary layer (PCF) and zero mean velocity gradient near a wall (SFCF), respectively. These two cases are considered as building-block flows since most turbulence models are based on the wall-layer similarity with a constant shear stress τ (Townsend 1976, §§5.4, 5.7–5.9). It is of our interest to characterize organized turbulence structures in the near-wall regions at different mean shear rates and to examine the capability of the current scaling laws (or turbulence models) in describing turbulence characteristics of such flows (cf. El Telbany & Reynolds 1980, 1981).

The purpose of Project **B** is to investigate the behavior of homogeneous turbulence subjected to axisymmetric distortion (contraction and expansion) and dilatation (Lee 1988). Closed-form solutions obtained by using RDT are compared with the numerical simulations (Lee & Reynolds 1985). The theoretical results are then used to develop a model for the pressure–strain-rate term $T_{ij} = (2/\rho)\overline{ps_{ij}}$. A 'simple' model for the pressure–strain-rate term shows that the 'history effect' (total strain) is important.

Project **C** is to explore detailed processes of the pressure–strain energy transfer in a turbulent shear flow (Brasseur & Lee 1987, 1988). Relationships between a local energy transfer event and the nearby vortical structures are studied by looking into instantaneous flow fields from numerical simulations of homogeneous shear flow (Rogers *et al.* 1986). For a kinematical description of the process, the energy transfer is classified into six classes according to the instantaneous directionality of the energy transfer between components. This concept of the energy transfer class can be applied to the statistical quantities such as the average value and probability density function (pdf). In this project, we are also interested in exploring the energy transfer across the different scales (e.g. spectral energy transfer) and its relationship with the intercomponent energy transfer.

2. Accomplishments

2.1. *Project* A*: Wall Turbulence*

2.1.1. *USBL Project*

The USBL project (Lee & Hunt 1988) convincingly demonstrates that the streak generation is entirely due the high shear rate, and that the surface blocking, in fact, prohibits formation of the streaks. As shown by Lee, Colonius &

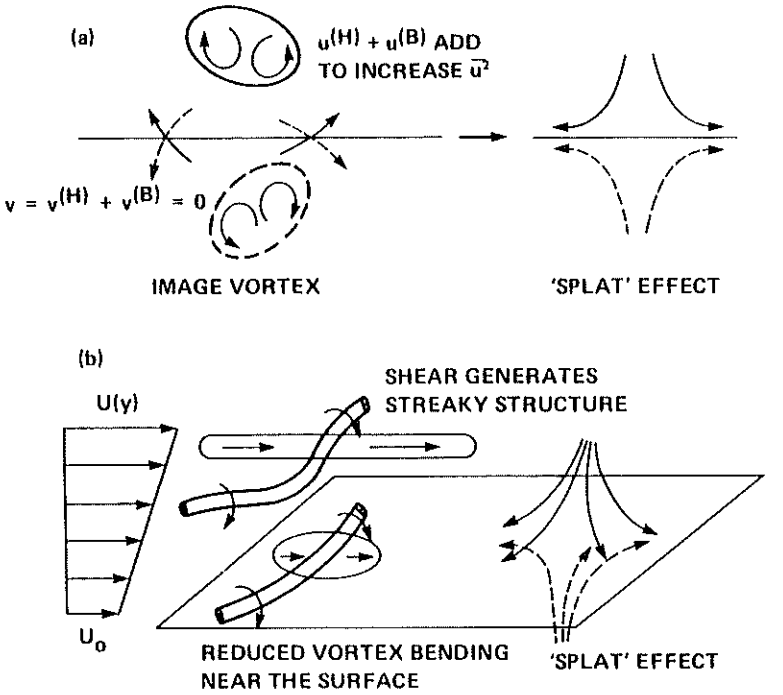

FIGURE 2. Schematic diagram to show difference between the mechanisms for (*a*) shear-free boundary layer, where image vortex below $y = 0$ induces irrotational velocity $\mathbf{u}^{(B)}$ above $y = 0$; and (*b*) uniform-shear boundary layer, where reduced vortex bending near the surface reduces $\overline{u^2}$ while splat effect increases $\overline{u^2}$.

Moin (1988), the streaks consist of eddies of large streamwise velocity fluctuations and turbulent shear stress $-uv$, and hence they are energy-producing eddies. The vorticity field associated with the streaks is found to be corrugated sheet vortex which has large spanwise and normal vorticity fluctuations, ω_z and ω_y, but relatively weak streamwise vorticity, ω_x. Near a solid surface, the corrugated vortex sheet becomes flat (less corrugated) due to the blocking effect of the surface, thus reducing the dominance of the streamwise fluctuations (see figure 2).

Figure 3 shows the energy spectra of the streamwise velocity $E_{11}(\kappa_3; y)$ as a function of the spanwise wavenumber κ_3 and total shear $\beta = St$ at $y/L = 0$ and 1 (L is the energy integral scale at $\beta = 0$). While there is no evident sign of the streaks at the surface $y = 0$ (fig. 3*a*), the spectra away from the surface ($y/L = 1$) show peaks that develop significantly with shear (fig. 3*b*). The fact that the streaks exist in sheared turbulence, independent of the presence of a solid boundary, but not in a shear-free boundary layer (Uzkan & Reynolds 1967), strongly supports the assertion that the main mechanism of generating

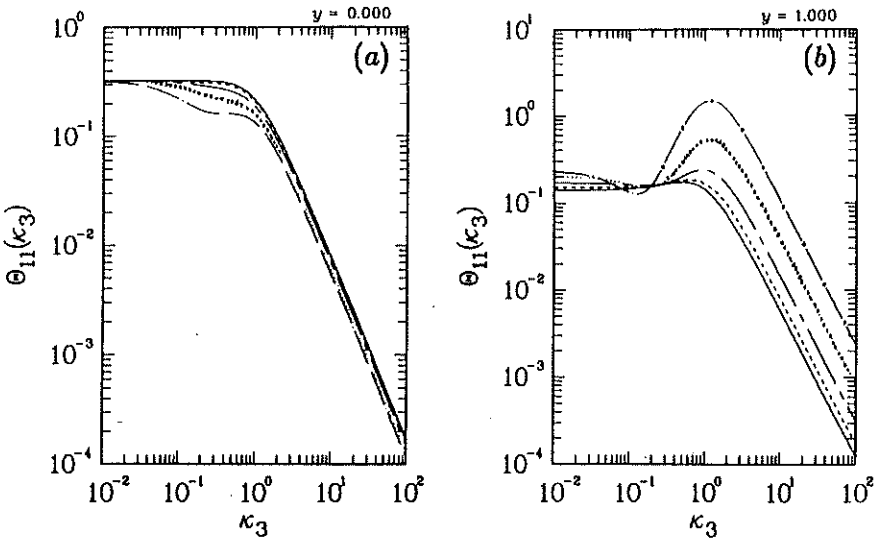

FIGURE 3. Variation with shear of the spanwise one-dimensional energy spectra $\Theta_{11}(\kappa_3)$ of the streamwise fluctuation: (*a*) $y = 0.0$; (*b*) $y = 1.0$. ——, $\beta = 0$; ----, $\beta = 1$; — — —, $\beta = 2$; ····· , $\beta = 4$; —·—, $\beta = 8$.

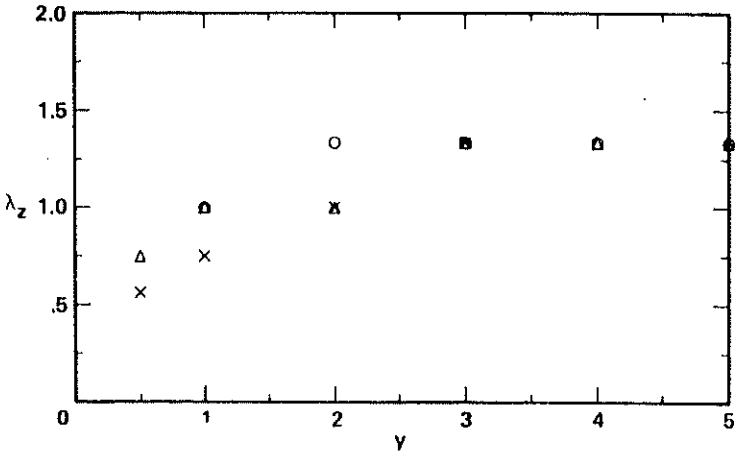

FIGURE 4. Variation with the distance from the boundary of the mean streak spacing, λ_z. The mean streak spacing is determined from the spanwise wavenumber at which $\Theta_{11}(\kappa_3; y)$ peaks. ○, $\beta = 2$; △, $\beta = 4$; ×, $\beta = 8$.

the streaks is the mean shear but not the wall blocking (Lee *et al.* 1987).

Notice that the peaks within a narrow band of κ_3 are indicative of the existence of the streaks in the flow. The mean spanwise spacing λ_z of the streaks can be estimated from the wavenumber at which the spectrum peaks: $\lambda_z = 1/\kappa_3^*$. In

figure 4, the variation of the mean streak spacing shows an increase with y. This study reinforces our earlier work (Lee, Kim & Moin 1987), namely, that the generation mechanism of the streaks is essentially *inviscid* and *linear*.

2.1.2. *PCF Project*

The PCF and SFCF projects make use of numerical databases from direct simulations. We have completed numerical simulation of plane Couette flow (PCF) with a wall moving at a speed U_w parallel to the stationary wall. The computation was performed on a $128 \times 129 \times 128$ grid and a passive scalar field ($\mathrm{Pr} = 0.71$) with constant boundary conditions was included in the computation. The flow Reynolds number Re based on the wall velocity U_w and half the channel width h is 6,000, and that based on the shear velocity $U_\tau = (\nu dU/dy|_w)^{1/2}$ is about 200. Other major aspects of the computation are similar to those in the Poiseuille flow of Kim *et al.* (1987). The computation has been conducted for a period of about 100 h/U_w that corresponds to about ten (10) computational box lengths.

In figure 5(a), the computed mean velocity profile across the channel is compared with the experimental results conducted at different flow Reynolds numbers ($\mathrm{Re} = 2{,}900$, Reichardt 1959; $\mathrm{Re} \simeq 2\times10^4 - 4\times10^4$, El Telbany & Reynolds 1980). It should be noticed that at high Reynolds numbers the velocity profile changes rapidly within a narrow region near the walls ($|y| \geq 0.8$), and that there exists a constant slope over half the channel width around the center ($|y| \leq 0.5$). The mean velocity gradient at the boundary $dU/dy|_w$ grows significantly with the Reynolds number. The near-wall profile made dimensionless by the viscous units (U_τ and $\ell_\nu = \nu/U_\tau$) is in good agreement with the classical law of the wall (fig. 5b).

The turbulence intensities (u'^+, v'^+, w'^+) scaled by the shear velocity U_τ in figure 6 also show good agreement with the experimental results at higher Reynolds numbers (El Telbany & Reynolds 1981). Compared with those in a plane Poiseuille flow at comparable Reynolds numbers (Kim *et al.* 1987; Kreplin & Eckelmann 1979), the intensities in PCF are significantly higher over most of the channel, except in the vicinity of the wall ($y \leq 30$) where the PCF values are only slightly higher. This marked contrast is a direct consequence of the constancy of total shear stress $\tau/\rho = \nu dU/dy - \overline{uv}$ across the channel in PCF. (In a plane Poiseuille flow, the total shear stress has a linear profile $\tau/|\tau_w| = -y/h$, and $dU/dy = 0$ and $\overline{uv} = 0$ at the channel center, $y = 0$, by symmetry.)

The turbulence structure exhibits strong anisotropy; even in the core region, $\overline{u^2} : \overline{v^2} : \overline{w^2} \simeq 6 : 1 : 2$. The linear mean velocity profile (i.e. constant mean shear rate) in the core region is indicative of the existence of homogeneous turbulence, where the turbulence statistics are approximately constant (see figure 6).

2.1.3. *SFCF Project*

In order to achieve zero mean shear rate in the wall region of shear-free channel flow (SFCF), one needs to determine the speed of the moving wall U_w and the

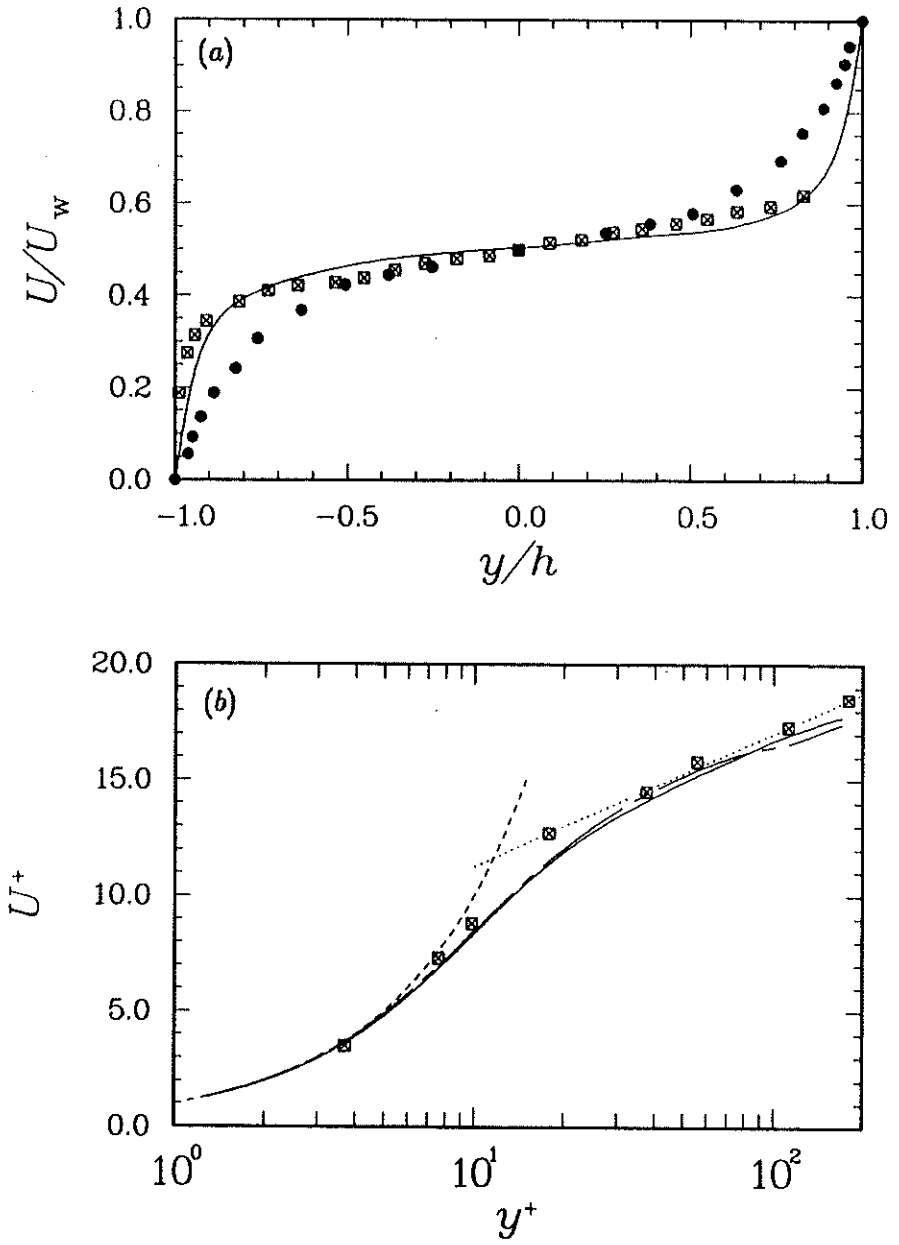

FIGURE 5. Mean velocity profile in plane Couette flow: (*a*) global profile, U/U_w *vs.* y/h; (*b*) near-wall profile, U^+ *vs.* y^+. ——, present result; ●, Reichardt (1959); ⊠, El Telbany & Reynolds (1980); ----, $U^+ = y^+$; ·····, $U^+ = (1/\kappa)\ln y^+ + B$ ($\kappa = 0.4$ and $B = 5.5$); In (*b*), the solid and chain-dashed lines are results for the lower and upper walls, respectively.

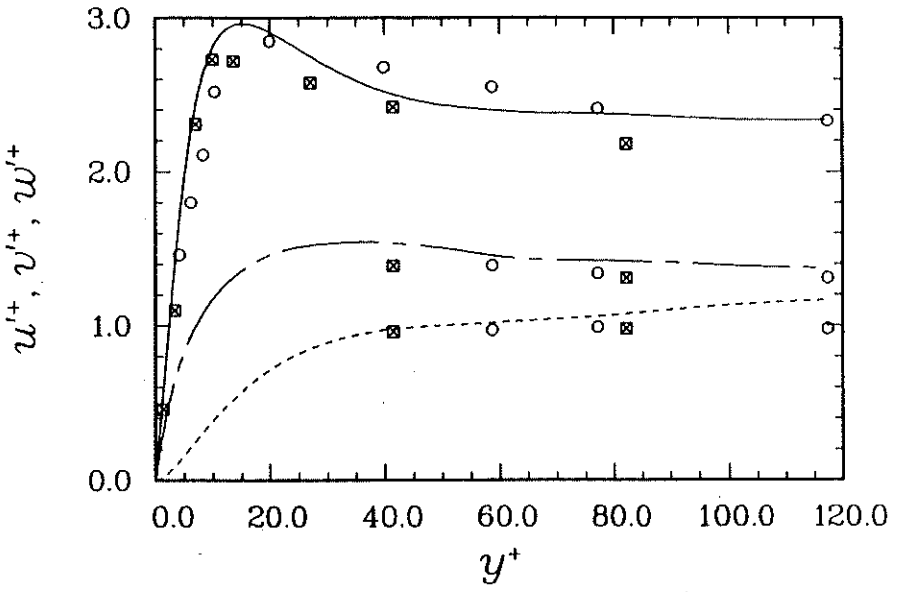

FIGURE 6. Near-wall profiles of the turbulence intensities in plane Couette flow: (u'^+, v'^+, w'^+) *vs.* y^+. Lines are present computation: ——, u'^+; - - - -, v'^+; — — —, w'^+. Symbolds are from El Telbany & Reynolds (1981): ○, Re = 19,000; ⊠, Re = 29,000.

constant pressure gradient dP/dx (see figure 1), which can be obtained only by solving the equations. Preliminary calculation on a $64 \times 129 \times 64$ grid has been carried with a developed plane Couette flow field as its initial condition; the value of the pressure gradient was varied at each timestep to obtain zero mean shear on the moving wall, and the response of the flow to the varying pressure gradient was found to be slow. Full-scale computation on a $128 \times 129 \times 128$ grid is planned.

2.2. *Project* B*: Axisymmetric-strain/Dilatation RDT*

Exact expressions for turbulence structural quantities, such as the Reynolds stresses and vorticity correlations, were obtained in closed form by using rapid distortion theory (Lee 1988). Comparison with the numerical simulations (Lee & Reynolds 1985) at a high strain rate shows remarkable agreement for all the quantities considered. Differences in effects of the two opposite, axisymmetric strain modes (contraction and expansion) on turbulence structure were investigated in detail. For example, axisymmetric contraction produces much higher fluctuation in velocity and vorticity ($R_{ij} = \overline{u_i u_j}$ and $V_{ij} = \overline{\omega_i \omega_j}$, respectively) as well as their anisotropy ($b_{ij} = R_{ij}/R_{kk} - \delta_{ij}/3$ and $v_{ij} = V_{ij}/V_{kk} - \delta_{ij}/3$, respectively) than does axisymmetric expansion. Figures 7(a, b) show comparison of anisotropy development during axisymmetric distortion.

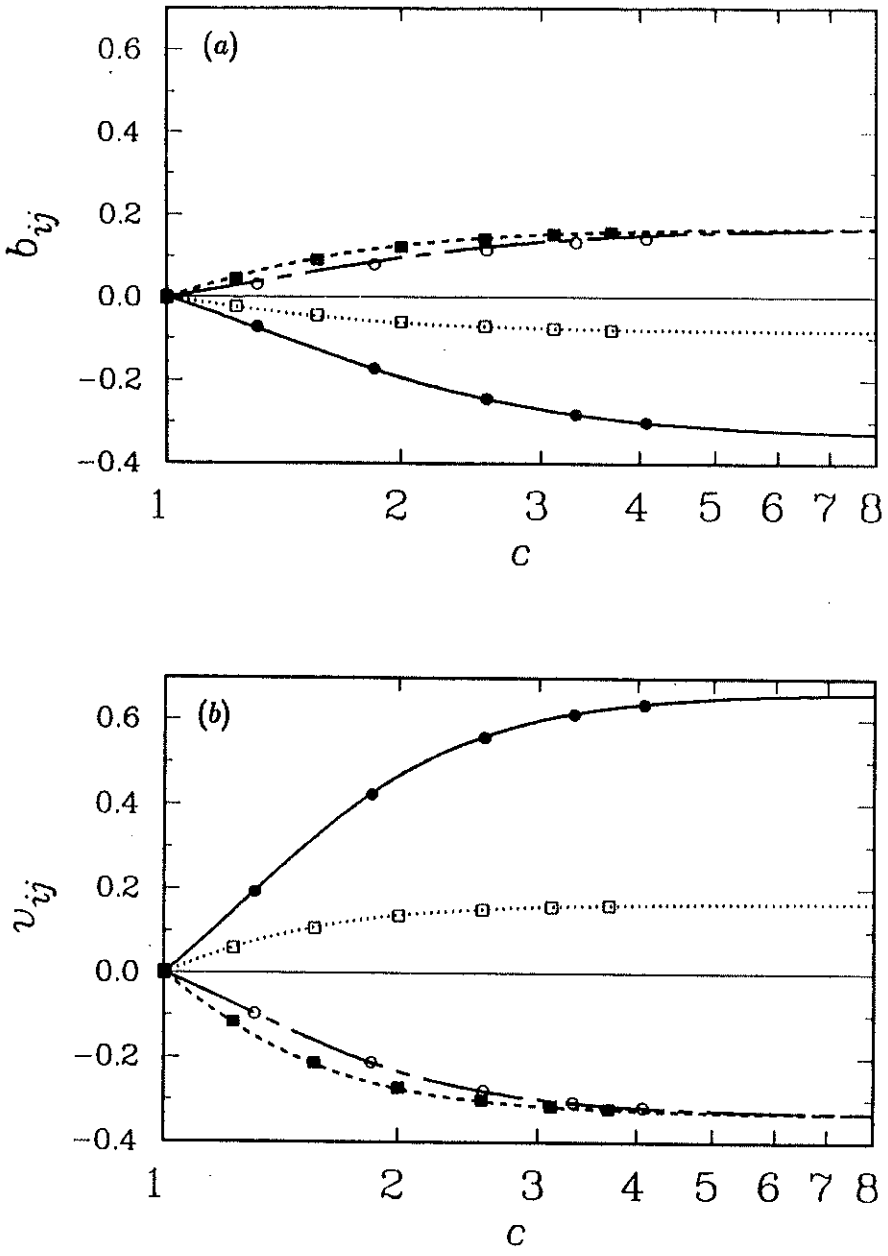

FIGURE 7. Evolution of anisotropy in axisymmetric strain flows (AC, axisymmetric contraction; AE, axisymmetric expansion): (*a*) Reynolds-stress anisotropy b_{ij}; (*b*) vorticity anisotropy, v_{ij}. Lines are RDT results: AC, ——, $i=1,j=1$; — — —, $i=2,j=2$; AE, - - - -, $i=1,j=1$; ·····, $i=2,j=2$. Symbols are from numerical simulations (Lee & Reynolds 1985): AC, ●, $i=1,j=1$; ○, $i=2,j=2$; AE, ■, $i=1,j=1$; □, $i=2,j=2$.

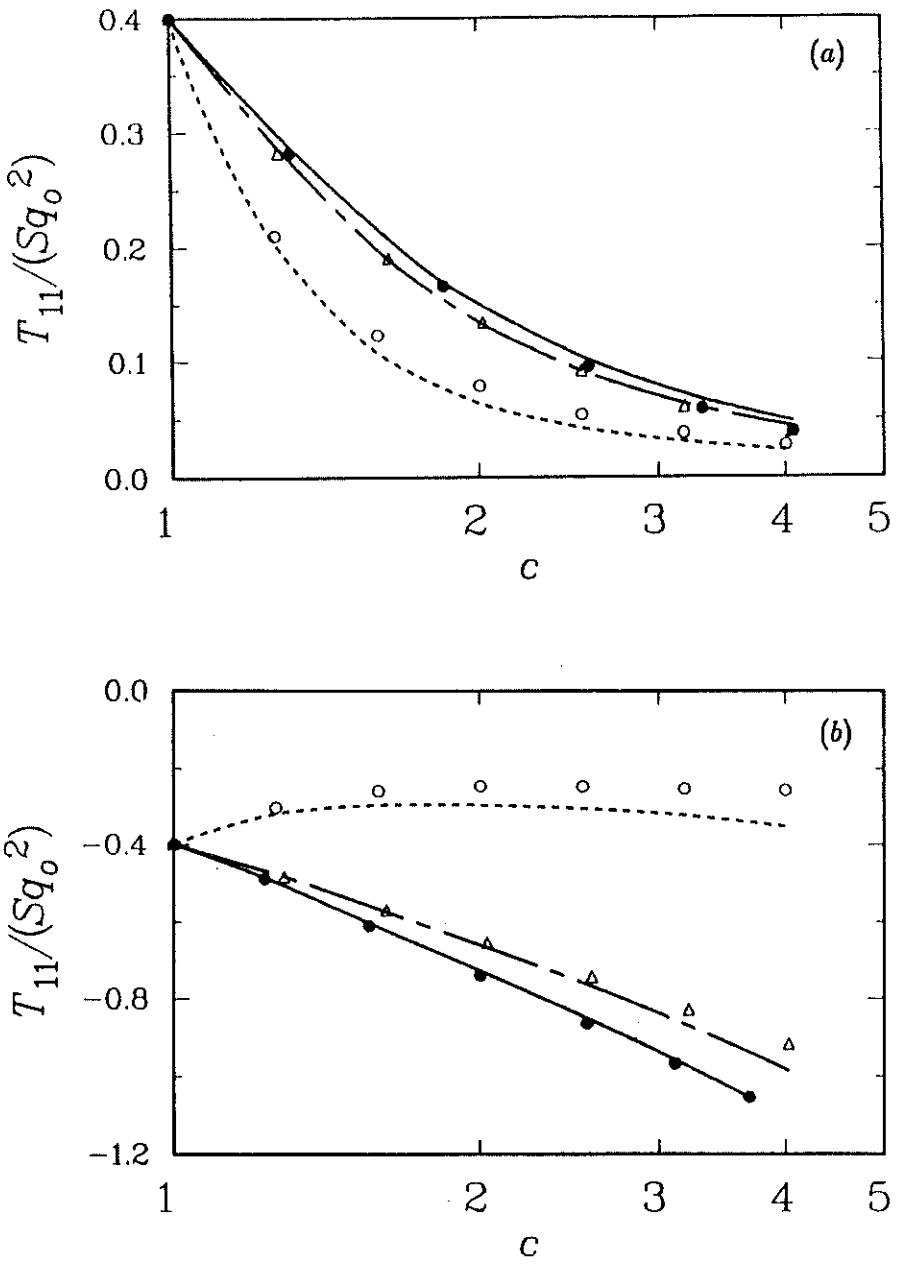

FIGURE 8. Test of the present model against different strain-rate cases, $T_{11}/(Sq_o^2)$: (*a*) axisymmetric contraction ($S_{11} > 0$); (*b*) axisymmetric expansion ($S_{11} < 0$). Lines are prediction of the present model and symbols are from numerical simulations (Lee & Reynolds 1985): —— and ●, $S^* \simeq 100$; – – – and △, $S^* \simeq 10$; ····· and ○, $S^* \simeq 1$.

The effect of mean-field dilatation on turbulence is also of interest. It is shown that, for flows of uniform, time-dependent density $\rho(t)$ at low turbulence Mach number, the statistical correlations, such as the 'Reynolds stress' $R_{ij} = \overline{u_i u_j}$, are related to those in the equivalent incompressible flow by a decomposition of mean strain-rate tensor, e.g. $R_{ij}(\mathbf{e}) = (\rho/\rho_0)^{2/3} R^*_{ij}(\mathbf{e}^*)$ where $e_{ij} = \int_0^t U_{i,j}(t')\,dt'$ is the total-distortion tensor and e^*_{ij} is the corresponding incompressible distortion (ρ_0 is the initial density). Similarly, the vorticity correlation $V_{ij} = \overline{\omega_i \omega_j}$ is given by $V_{ij}(\mathbf{e}) = (\rho/\rho_0)^{4/3} V^*_{ij}(\mathbf{e}^*)$. It was also found that the rate of dilatation does not contribute to pressure fluctuation.

Terms in the transport equation for R_{ij} were evaluated for axisymmetric strain flow, and existing models for the pressure–strain-rate term were examined. It was shown that improvements can be made for the model by incorporating structural parameters based on the linear analysis (RDT) of axisymmetric strain flows. Prediction of the improved model agrees quite well with the numerical simulations, even in cases at lower strain rates (figure 8). This study indicates that a turbulence model should reflect 'history effect,' since a state in nonstationary turbulence depends not only on the instantaneous quantities (e.g. the Reynolds stresses) but also on the memory effect (e.g. total strain) accumulated during a distortion.

2.3. *Project* C*: Energy Transfer Process*

A detailed study of the intercomponent energy transfer processes by the pressure–strain-rate in homogeneous shear flow has been carried out by using a numerical database by Rogers *et al.* (1986). In the previous study (Brasseur & Lee 1987), it was found that the rapid and slow parts of fluctuating pressure are uncorrelated, i.e. $\overline{p_r p_s}/(\overline{p_r^2}\,\overline{p_s^2})^{1/2} \ll 1$, and their scales are widely separated, providing a strong justification for current modeling procedure in which the pressure–strain-rate term is split into the corresponding parts. It was shown that local intercomponent energy transfer processes are associated with high vorticity regions. We limit our discussion to the 'slow' pressure–strain-rate $\phi_{ij} = (2/\rho)\,\overline{p_s s_{ij}}$.

Our recent study (Brasseur & Lee 1988) of probability density functions (pdf's) and contour plots of the pressure–strain-rate shows that the energy transfer processes are extremely peaky (figure 9), with high-magnitude events dominating low-magnitude fluctuations, as reflected by very high flatness factors (30–40). The concept of the energy transfer class is defined as

$$\mathbf{C}^{\pm\pm\pm} = \{\phi_{ij}(\mathbf{x}, t) \,|\, \phi_{11} \gtrless 0, \phi_{22} \gtrless 0, \phi_{33} \gtrless 0\}.$$

For example, $\mathbf{C}^{-++}$ denotes the class of ϕ_{ij} in which energy leaves u ($\phi_{11} < 0$) and enters v and w ($\phi_{22} > 0$, $\phi_{33} > 0$). Note that this classification of the energy transfer is unique and there are six possible classes which are disjoint (or mutually exclusive). The classification has been applied to investigate details of

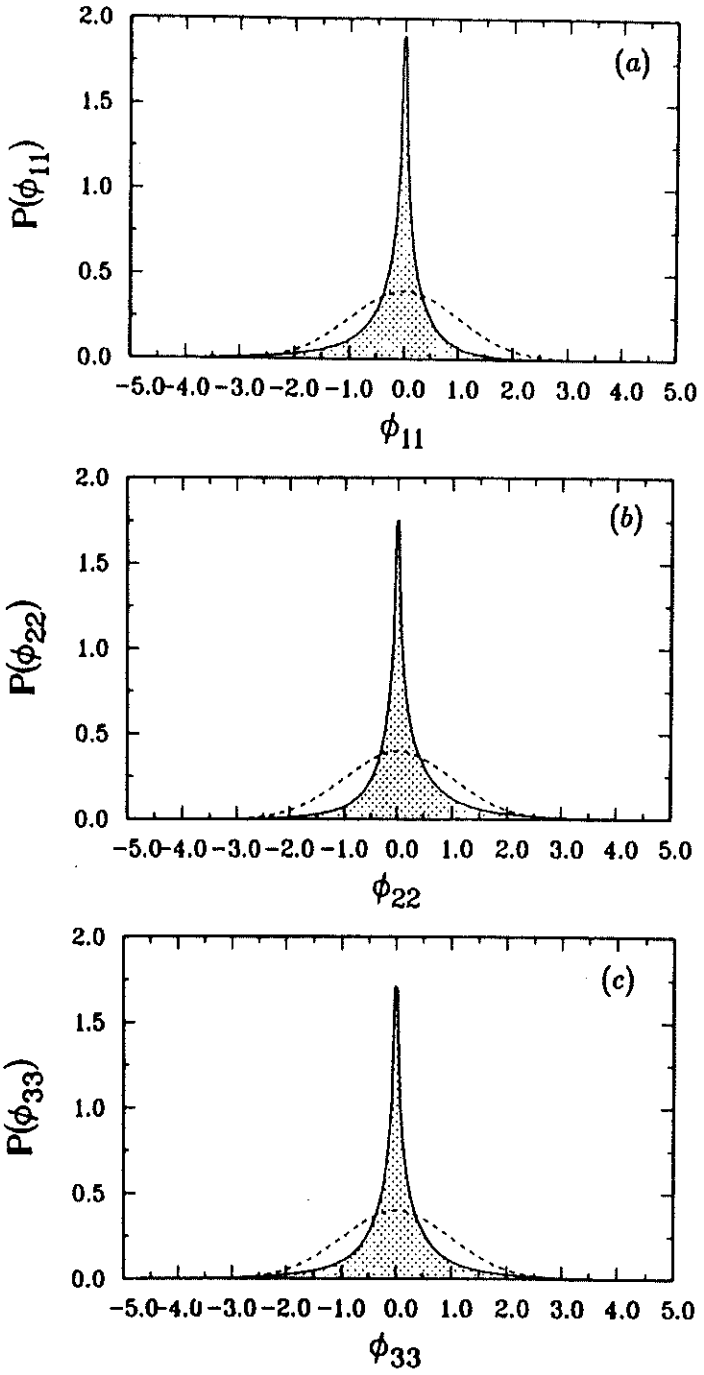

FIGURE 9. Pdf's of the diagonal elements of the slow pressure–strain-rate $\phi_{ij} = ps_{ij}$: (*a*) $P(\phi_{11})$; (*b*) $P(\phi_{22})$; (*c*) $P(\phi_{33})$. ----, Gaussian distribution.

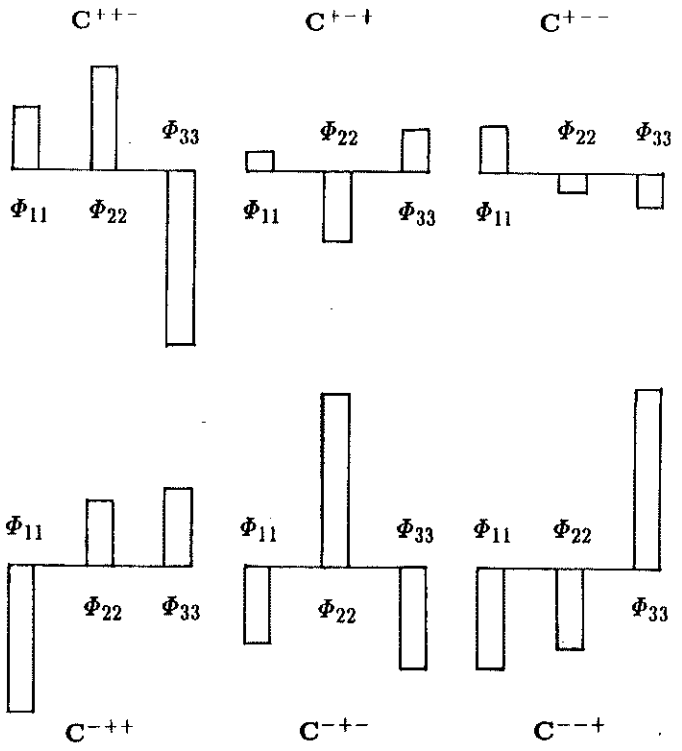

FIGURE 10. Schematic of the intercomponent energy transfer processes, representing contributions from all magnitudes of ϕ_{ij} events. The schematic shows that the four classes $\mathbf{C}^{++-}$, $\mathbf{C}^{-++}$, $\mathbf{C}^{-+-}$ and $\mathbf{C}^{--+}$ are dominant.

the direction as well as magnitude of the energy transfer processes. Examination of contours in an instantaneous field, pdf's and weighted pdf's of the pressure–strain-rate indicates that in the low-magnitude regions (defined as where $|\phi_{\alpha\alpha}| <$ 1.5 r.m.s. $\phi_{\alpha\alpha}$) all six classes are important, but in the high-magnitude regions four classes $\mathbf{C}^{++-}$, $\mathbf{C}^{-++}$, $\mathbf{C}^{-+-}$ and $\mathbf{C}^{--+}$ dominate. The contribution to the average slow pressure–strain-rate from the high-magnitude fluctuations is only 50% or less, indicating complexity of the problem. However, when summed over all magnitudes, the same four classes of energy transfer dominate as shown by the schematic in figure 10.

3. Future Plan

3.1. *Project* A*: Wall Turbulence*

3.1.1. *USBL Project*

We plan to look into other aspects of the blocking effect of the boundary by examining the two-point correlations between the vertical velocity component

and the streamwise and vertical components. Here, we are interested in assessing the degree of self-similarity of these correlations and seeking possible scaling laws that can be used to develop near-wall turbulence models.

3.1.2. *PCF Project*

It is anticipated to learn a great deal about how the turbulence structure changes across the interface between the homogeneous core region and inhomogeneous wall region. We are especially interested in examining the structure of *stationary, homogeneous, sheared turbulence* in the core region. The *stationarity and homogeneity* in this flow are generated in a *natural* way, unlike in flows where artificial forcing techniques are used.

3.1.3. *SFCF Project*

The SFCF project complements the USBL and PCF studies in many respects. While the USBL and PCF projects focus on the role of the mean shear rate in affecting structure of turbulence in wall layer, the SFCF study is designed to study the kinematical nature of the presence of a boundary, i.e. the inquiry into how turbulence is suppressed by the boundary. We expect to learn details of physical mechanisms involving energy redistribution near the boundary, and comparison will be made between the RDT study of shear-free boundary layer, a special case of USBL at $\beta = 0$ (Lee & Hunt 1988). Another impetus to carry out the SFCF project is that this flow allows a unique opportunity to develop a turbulence model for the transport terms, since, in the shear-free wall layer, the transport terms balance the dissipation term in the equation for turbulent kinetic energy.

3.2. *Project C: Energy Transfer Process*

Inspection of the energy transfer processes depicted in figure 10 poses an interesting question about the kinematic structure of the energy transfer. It appears that the dominant energy transfer to or from one component is provided by the other two components. If the off-diagonal components in ϕ_{ij} are negligible, then most of the energy transfer takes place within axisymmetric flow regimes. The answer awaits invariant analysis of the tensorial structure of the pressure–strain-rate (and strain rate).

In parallel with the intercomponent energy transfer, energy transfer between scales in a flow with coherent vortical structures is also important. In an attempt to generate coherent structures in grid turbulence, Michard *et al.* (1987) used a grid with propellers which give rise to spectral disturbances. Their study showed that the initially strong anisotropy near the grid due to spectral disturbances relaxes to an axisymmetric state. Numerical simulation is planned to investigate such a flow. We are interested in looking into how the disturbances are transferred between components as well as between scales.

Acknowledgements

I would like to acknowledge support from the Center for Turbulence Research. I have been benefitted from many helpful discussions with J. G. Brasseur, J. C. R. Hunt, J. Kim, P. Moin and W. C. Reynolds.

REFERENCES

BRASSEUR, J. G. & LEE, M. J. 1987 Local structure of intercomponent energy transfer in homogeneous turbulent shear flow. *Proc. Summer Program 1987*, pp. 165–178. Ctr. for Turb. Res., Stanford Univ. and NASA-Ames Res. Ctr.

BRASSEUR, J. G. & LEE, M. J. 1988 Pressure–strain-rate events in homogeneous turbulent shear flow. *Proc. Summer Program 1988*, pp. 143–156. Ctr. for Turb. Res., Stanford Univ. and NASA-Ames Res. Ctr.

EL TELBANY, M. M. M. & REYNOLDS, A. J. 1980 Velocity distributions in plane turbulent channel flows. *J. Fluid Mech.* **100**, 1–29.

EL TELBANY, M. M. M. & REYNOLDS, A. J. 1981 Turbulence in plane channel flows. *J. Fluid Mech.* **111**, 283–318.

HUNT, J. C. R. 1984 Turbulence structure in thermal convection and shear-free boundary layers. *J. Fluid Mech.* **138**, 161–184.

HUNT, J. C. R. & GRAHAM, J. M. R. 1978 Free-stream turbulence near plane boundaries. *J. Fluid Mech.* **84**, 209–235.

KIM, J., MOIN, P. & MOSER, R. D. 1987 Turbulent statistics in fully developed channel flow at low Reynolds number. *J. Fluid Mech.* **177**, 133–166.

KLINE, S. J., REYNOLDS, W. C., SCHRAUB, F. A. & RUNSTADLER, P. W. 1967 The structure of turbulent boundary layers. *J. Fluid Mech.* **30**, 741–773.

KREPLIN, H. & ECKELMANN, H. 1979 Behavior of the three fluctuating velocity components in the wall region of a turbulent channel flow. *Phys. Fluids* **22**, 1233.

LEE, M. J. 1988 Distortion of homogeneous turbulence by axisymmetric strain and dilatation. (Manuscript in preparation for publication.)

LEE, M. J., COLONIUS, T. & MOIN, P. 1988 The vorticity field associated with the steaks in turbulent shear flows. *Bull. Amer. Phys. Soc.*, **33**(10), 2229.

LEE, M. J. & HUNT, J. C. R. 1988 The structure of sheared turbulence near a plane boundary. *Proc. Summer Program 1988*, pp. 221–241. Ctr. for Turb. Res., Stanford Univ. and NASA-Ames Res. Ctr.

LEE, M. J., KIM, J. & MOIN, P. 1987 Turbulence structure at high shear rate. In *Sixth Symp. on Turbulent Shear Flows*, Toulouse, France, Sept. 7–9, 1987 (ed. F. Durst *et al.*), pp. 22.6.1–22.6.6.

LEE, M. J. & REYNOLDS, W. C. 1985 Numerical experiments on the structure of homogeneous turbulence. *Dept. Mech. Engng. Rep.* TF–24, Stanford University: Stanford, California.

MICHARD, M., MATHIEU, J., MOREL, R., ALCARAZ, E. & BERTOGLIO, J. P. 1987 Grid-generated turbulence exhibiting a peak in the spectrum. *Advances in Turbulence*, Proc. First Euro. Turb. Conf., Lyon, France, July 1–4, 1986 (ed. G. Comte-Bellot & J. Mathieu), pp. 163–169. Springer-Verlag: Berlin.

REICHARDT, H. 1959 Gesetzmäßigkeiten der geradlinigen turbulenten Couettesträmung. Mitt. Max-Planck-Inst. Strömungsforschung und Aerodynamischen Versuchsanstalt, No. 22.

ROGERS, M. M., MOIN, P. & REYNOLDS, W. C. 1986 The structure and modeling of the hydrodynamic and passive scalar field in homogeneous turbulent flows. *Dept. Mech. Engng. Rep.* TF–25, Stanford University: Stanford, California.

TOWNSEND, A. A. 1976 *The structure of turbulent shear flows.* 2nd edn. Cambridge University Press: Cambridge, England.

UZKAN, T. & REYNOLDS, W. C. 1967 A shear-free turbulent boundary layer. *J. Fluid Mech.* **28**, 803–821.